

Conditional Depletion of Airway Progenitor Cells Induces Peribronchiolar Fibrosis

Anne-Karina T. Perl¹, Dieter Riethmacher², and Jeffrey A. Whitsett¹

¹Division of Pulmonary Biology, Perinatal Institute, Cincinnati Children's Hospital Medical Center, Cincinnati, Ohio; and ²Human Genetics Division, University of Southampton, School of Medicine, Southampton, United Kingdom

Rationale: The respiratory epithelium has a remarkable capacity to respond to acute injury. In contrast, repeated epithelial injury is often associated with abnormal repair, inflammation, and fibrosis. There is increasing evidence that nonciliated epithelial cells play important roles in the repair of the bronchiolar epithelium after acute injury. Cellular processes underlying the repair and remodeling of the lung after chronic epithelial injury are poorly understood.

Objectives: To identify cell processes mediating epithelial regeneration and remodeling after acute and chronic Clara cell depletion.

Methods: A transgenic mouse model was generated to conditionally express diphtheria toxin A to ablate Clara cells in the adult lung. Epithelial regeneration and peribronchiolar fibrosis were assessed after acute and chronic Clara cell depletion.

Measurements and Main Results: Acute Clara cell ablation caused squamous metaplasia of ciliated cells and induced proliferation of residual progenitor cells. Ciliated cells in the bronchioles and pro-surfactant protein C-expressing cells in the bronchiolar alveolar duct junctions did not proliferate. Epithelial cell proliferation occurred at multiple sites along the airways and was not selectively associated with regions around neuroepithelial bodies. Chronic Clara cell depletion resulted in ineffective repair and caused peribronchiolar fibrosis.

Conclusions: Colocalization of proliferation and cell type-specific markers demonstrate that Clara cells are critical airway progenitor cells. Continuous depletion of Clara cells resulted in persistent squamous metaplasia, lack of normal reepithelialization, and peribronchiolar fibrosis. Induction of proliferation in subepithelial fibroblasts supports the concept that chronic epithelial depletion caused peribronchiolar fibrosis.

Keywords: chronic obstructive pulmonary disease; bronchiolitis obliterans syndrome; squamous metaplasia; diphtheria toxin; progenitor cells

After an acute injury the respiratory epithelium is capable of remarkable regeneration without remodeling or fibrosis. The importance of nonciliated bronchiolar epithelial cells (Clara cells) in the peripheral airways and basal cells in the cartilaginous airways in repair after acute injury has been supported by findings in mouse models (1–8). It remains unclear whether all Clara cells, or only restricted subpopulations, have the capacity to self-renew, differentiate, and repopulate the conducting airway epithelium. Previous studies that directly test whether repeated depletion of Clara cells exhaust bronchiolar stem cell pools were limited by insufficient long-term survival after chronic Clara cell depletion (2, 6).

(Received in original form May 11, 2010; accepted in final form September 23, 2010)

Supported by NIH grant HL 090156 (J.A.W., A.K.P.) and ALA RG-123729-N (A.K.P.).

Correspondence and requests for reprints should be addressed to Anne-Karina Perl, Ph.D., Children's Hospital Medical Center, Divisions of Neonatology and Pulmonary Biology, 3333 Burnet Avenue, Cincinnati, OH 45229-3039. E-mail: Anne.Perl@cchmc.org

This article has an online supplement, which is available from the issue's table of contents at www.atsjournals.org

Am J Respir Crit Care Med Vol 183, pp 511–521, 2011

Originally Published in Press as DOI:10.1164/rccm.201005-0744OC on September 24, 2010
Internet address: www.atsjournals.org

AT A GLANCE COMMENTARY

Scientific Knowledge on the Subject

Nonciliated bronchiolar epithelial cells participate in the repair of the airway after acute injury. In humans, successive lung injury and failure to repair the respiratory epithelium are associated with fibrosis as seen in idiopathic pulmonary fibrosis, bronchiolitis obliterans, and other lung diseases, and suggest that the epithelial cells fail to repair the damaged epithelium because of ineffective proliferation, migration, and differentiation.

What This Study Adds to the Field

We provide evidence that repeated injury to nonciliated bronchiolar epithelial cells is sufficient to cause pulmonary fibrosis at sites of insufficient repair and reepithelialization.

In sharp contrast to rapid repair after acute lung injury, chronic injury results in structural remodeling of lung tissue, commonly associated with chronic lung diseases, including asthma, chronic bronchitis, chronic obstructive pulmonary disease (COPD), and bronchiolitis obliterans syndrome (BOS) (9–12). A better understanding of the cellular and molecular processes mediating bronchiolar regeneration, as well as the pathogenesis of fibrosis after loss of epithelial integrity, is needed to develop effective therapeutic strategies for chronic pulmonary disorders. Histological evaluation of human biopsies support the concept that pulmonary fibrosis is caused by failure of epithelial repair due to ineffective proliferation, migration, and differentiation (13); these findings are supported by animal models that demonstrate the importance of airway homeostasis and the role of epithelial cell injury in the pathogenesis of pulmonary fibrosis (14–16). It remains unclear whether transdifferentiation of alveolar type II cells to mesenchymal cells (epithelial–mesenchymal transition, EMT) or migration of nonpulmonary cells into the lung plays an important role in the progression of pulmonary fibrosis (14, 15, 17).

Although many studies have suggested that injury of the alveolar epithelium causes pulmonary fibrosis, studies regarding the pathogenesis of bronchiolar fibrosis are limited. The present study was designed to develop a mouse model to conditionally deplete Clara cells to study bronchiolar regeneration after acute and chronic injury, and to test whether chronic Clara cell death results in ineffective repair, progenitor cell exhaustion, and fibrosis. We used the rat *Scgb1a1* (secretoglobin, family 1A, member 1) promoter to conditionally express a diphtheria toxin A gene (*DT-A*) causing cell autonomous death. Administration of doxycycline (dox) activates Cre recombinase in Clara cells, and initiates genomic recombination of an otherwise silent *DT-A* gene to cause cell death. Continuous Clara cell depletion caused peribronchiolar fibrosis and regional exhaustion of pro-

genitor cells. Portions of these results have been presented previously in abstract form (18).

METHODS

Additional detail on the methods is provided in the online supplement.

Transgenic Mice and Tissue Harvest

To achieve both Clara cell-specific and time-controlled expression of DT-A a triple transgenic mouse model was generated using the reverse tetracycline activator (rtTA), Cre recombinase, and a *loxP*-activated *DT-A* gene (5, 19–22). Dox was given to mice via their food (dox, 625 mg/kg chow; Harlan Teklad, Madison, WI) (23). Triple transgenic Scgb1a1rtTA/tetOCre/R26:lacZ/DT-A mice (termed Scgb1a1/DT-A hereafter) were used in all studies. Wild-type, single transgenic littermates and untreated triple transgenic mice served as controls. In the present study, two independent Scgb1a1rtTA founder lines (line 1 and line 2) were compared for their ability to target Cre and subsequent DT-A expression to Clara cells in the bronchiolar epithelium. Because Clara cell depletion was more extensive in Scgb1a1/DT-A mice of line 2, this line was used for subsequent acute and chronic injury studies. For acute lung injury studies, mice were treated with dox for 2 days. Chronic lung injury was induced by continued dox treatment for 10 days. Three to five animals per group were analyzed. Mice were killed by injection of 0.2–0.3 ml of anesthetic containing ketamine, xylazine, and acepromazine. Lungs were inflation-fixed with 4% paraformaldehyde, fixed overnight at 4°C, and processed for paraffin embedding. Peroxidase and fluorescence immunohistochemistry was performed on paraffin sections as previously described (24).

Mitotic Index and Proliferation in Neuroepithelial Bodies and Bronchiolar Alveolar Duct Junction Regions

The mitotic index was assessed by fluorescence immunohistochemistry for phosphohistone H3-positive cells or Ki67-positive nuclei. Six sections (spaced 80–100 μm apart) containing all five lobes, from three to five mice per group and time point, were double-labeled for Ki67 and calcitonin gene-related peptide (CGRP) and counterstained with 4',6-diamidino-2-phenylindole (DAPI). Per slide, five to seven random, nonoverlapping pictures (magnification, ×10) containing bronchiolar airways were photographed and analyzed with MetaMorph software (Molecular Devices, Sunnyvale, CA). Neuroepithelial body (NEB) regions were determined by positive CGRP staining. The number of positive cells per millimeter of airway and the percentage of positive cells per DAPI-positive cell in NEB and non-NEB regions were determined. Three sections of three to five animals per group and time point, containing all five lobes, were triple labeled for Ki67, pro-surfactant protein C (SPC), and Clara cell secretory protein (CCSP) and counterstained with DAPI. A minimum of 15 BADJ regions per animal were examined for colocalization of CCSP, pro-SPC, and Ki67.

Quantitative Analysis

Morphometric analysis for Clara cell depletion, extent of fibrosis, and extent of epithelial denudation was performed on random sections containing all five lobes of two or three mice per group. Nonoverlapping pictures of all airways on these slides were photographed and analyzed with MetaMorph software (Molecular Devices). The length of total airway epithelia and of CCSP-positive and pan-cytokeratin-positive airway epithelia was determined (goat anti-CCSP, diluted 1:5,000 [Santa Cruz Biotechnology, Santa Cruz, CA] and mouse anti-pan-cytokeratin, diluted 1:500 [Sigma, St. Louis, MO]). The area of mesenchymal tissue adjacent to the bronchiolar basement membrane was determined. Clara cell depletion was expressed as the percentage of airways covered with CCSP-positive cells. Extent of fibrosis was determined as area per millimeter of airway. Extent of epithelial denudation was expressed as the percentage of airway lacking pan-cytokeratin-positive staining, using light microscopy at ×40 magnification.

RESULTS

Conditional Expression of Diphtheria Toxin in Clara Cells

Cre-mediated activation of DT-A has been successfully used in other organs to deplete endocardial cells, dendritic cells, in-

testinal stem cells, cardiovascular smooth muscle cells, oligodendrocytes, B cells, and hepatocytes (25–29). This mouse model differs from prior studies in that Cre-mediated recombination was activated by the reverse tetracycline activator after dox treatment, enabling temporal and cell type-specific control of the DT-A expression in a subset of epithelial cells in the lung. We used two independent Scgb1a1rtTA mouse lines, line 1 (19) and line 2 (30), that vary in the extent to which Clara cells express Cre recombinase. Both lines were generated with a 2.3-kb rat *Scgb1a1* gene promoter. Cre expression in the bronchiolar epithelium was detected in both mouse lines, but was more widespread in line 2 (see Figure E1 in the online supplement). Transgenic Scgb1a1rtTA/tetOCre mice of lines 1 and 2 were mated to R26:lacZ/DT-A transgenic mice (21). In the triple transgenic progeny, Scgb1a1/DT-A, Cre recombination was activated by dox for 2 or 10 days to induce activation of DT-A causing acute or chronic Clara cell ablation, respectively (Figure E2).

Acute Clara Cell Depletion after 2 Days of DT-A Activation

To determine the timing and extent of Clara cell depletion after DT-A expression, morphological changes in the bronchiolar epithelium were assessed 2 days after exposure to dox and 2 days after withdrawal from dox (Figure 1). Histological changes in the bronchiolar epithelium were not detected after 2 days of dox treatment, but were readily detected 2 days after withdrawal from dox. Insufficient Clara cell targeting and ablation of a subset of Clara cells in line 1 resulted in Clara cell hyperplasia (Figure 1C). Increased proliferation in nontargeted Clara cells was confirmed by increased expression of phosphohistone H3 (inset in Figure 1B). Rapid cell replacement was seen in diphtheria toxin receptor-expressing dendritic cells but not in podocytes of the kidney (31, 32). This Clara cell hyperplasia suggests that “nontargeted” Clara cells or other progenitor cells respond to epithelial injury with rapid proliferation. A similar increase in cell proliferation has been shown in a different DT-A mouse model, in which the human diphtheria toxin receptor is expressed in alveolar type II cells (16). In contrast, in line 2, the majority of Clara cells in the lung bronchioles were ablated during dox treatment, leaving a squamous epithelium with rare clusters of cuboidal cells. Using two CCSP antibodies that differ in their sensitivity to detect CCSP protein, we determined that $4.5 \pm 2.0\%$ of the remaining cells expressed low levels of CCSP and were likely untargeted Clara cells or cells that were newly derived from bronchiolar progenitor cells after dox withdrawal (Figure 1F). Subsequent studies, to determine repair after acute and chronic Clara cell ablation, were performed in triple transgenic mice using Scgb1a1rtTA line 2.

Regeneration of Bronchiolar Cells after Acute Clara Cell Death

Hematoxylin and eosin staining and CCSP immunohistochemistry were used to assess histological changes after exposure of Scgb1a1/DT-A mice to 2 days of dox treatment and either 2, 5, or 10 days of subsequent repair (Figures 2A–2H). Most bronchiolar epithelial cells were still present in the bronchiolar epithelium 2 days after dox exposure (Figures 2A and 2E); this delay in cell death is likely due to dox pharmacodynamics, and the lag time between dox uptake, rtTA and Cre protein expression, DNA recombination, and activation of DT-A protein expression. However, during the subsequent 2 days more than $95.5 \pm 2.0\%$ of Clara cells were lost, leaving a squamous bronchiolar epithelium (Figures 2B and 2F). CCSP protein expression in these cells could be detected only with the more sensitive antibody to CCSP (Figure 2F), suggesting that all these Clara cells expressed low levels of CCSP protein. The percentage of Clara cells increased gradually after 5 days (Figures 2C

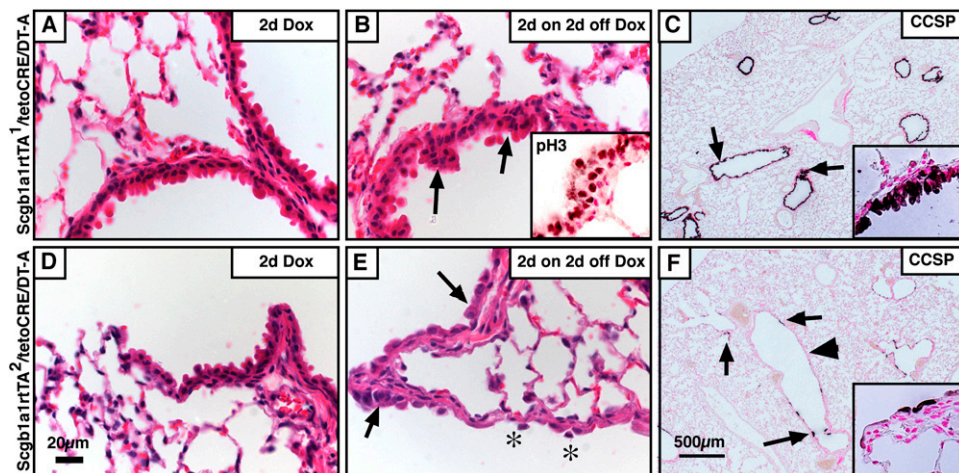


Figure 1. Clara cell depletion after acute doxycycline (dox) exposure: Hematoxylin and eosin staining of histological lung sections after (A and D) 2 days of dox exposure and (B and E) 2 days of dox exposure followed by 2 days of recovery in triple transgenic mice from (A–C) Scgb1a1rtTA line 1 and (D–F) Scgb1a1rtTA line 2. Immunohistochemistry for the proliferation marker phosphohistone H3 (pH3) revealed increased proliferation in Scgb1a1rtTA line 1 (inset in B); (C and F) immunohistochemistry using goat anti-Clara cell secretory protein (CCSP) revealed that $95.5 \pm 2.0\%$ of Clara cells were depleted after 2 days of dox exposure and 2 days of recovery. Arrows in B and C indicate bronchiolar hyperproliferation; arrows in E and F indicate clusters

of cuboidal cells; asterisks in E show cells sloughing off; the arrowhead in F shows a bronchiole depleted of Clara cells. Figures are representative of at least five individual mice per genotype and at each time. Scale bars: (A, B, D, and E) 20 μm ; (C and F) 500 μm .

and 2G). After 10 days, regenerating cells had formed larger clusters of Clara cells that stained intensively for CCSP and covered $45.5 \pm 16.2\%$ of the airways (Figure 2H). To determine whether remaining ciliated cells covered the basement membrane, we performed immunohistochemistry for β -tubulin (Figures 2I–2L). Despite extensive depletion of Clara cells, bronchiolar epithelial integrity was maintained as β -tubulin IV-expressing ciliated cells formed a squamous monolayer (Figures 2I–2L). These findings are consistent with previous observations after naphthalene-induced Clara cell injury (6, 33, 34).

Proliferation of Clara Cells But Not Ciliated Cells during Bronchiolar Regeneration

To determine the cell types contributing to regenerating cells in the bronchiolar epithelium, we colocalized the proliferation marker Ki67 with CCSP or FOXJ1 (forkhead-box J1) expression. To detect low levels of CCSP expression we used the more

sensitive goat anti-CCSP antibody in all immunofluorescence studies (Figure 3). Although generally nonproliferative, $8.5 \pm 4.4\%$ of the bronchiolar cells proliferated after 2 days, and $10.0 \pm 7.7\%$ proliferated after 5 days. Whereas a subset of proliferative cells expressed low levels of CCSP, a distinct subset of proliferative cells were cuboidal and lacked both CCSP and FOXJ1 expression (Figure 3D). Five days after withdrawal from dox, all Ki67-positive cells were CCSP positive and FOXJ1 never colocalized with Ki67 (Figures 3B, 3E, and 3H). FOXJ1 colocalized with CCSP in a subset of cells after 5 days of recovery, perhaps indicating differentiation of a subset of Clara cells into ciliated cells (Figure 3I).

Proliferation in Selected Cell Niches in the Bronchioles

Epithelial regeneration after naphthalene injury has been associated with a subpopulation of naphthalene-resistant Clara cells (variant Clara cells) that are located at selective stem cell

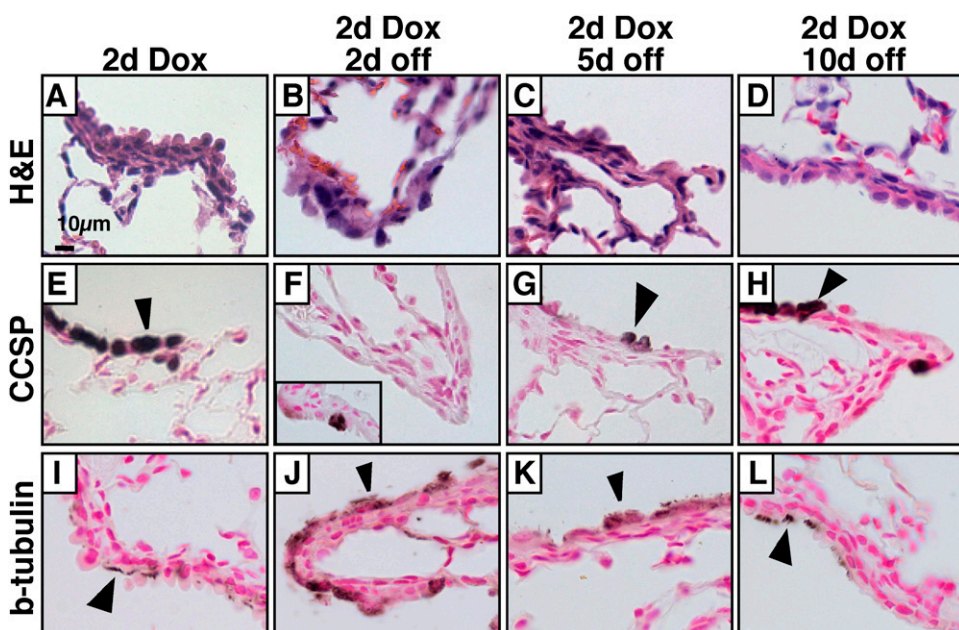


Figure 2. Residual squamous cells maintain the bronchiolar epithelium. (A, E, and I) Triple transgenic mice were exposed to doxycycline (dox) for 2 days to activate diphtheria toxin A (DT-A) by Cre recombination. Histology was assessed (B, F, and J) 2 days, (C, G, and K) 5 days, and (D, H, and L) 10 days after dox withdrawal, using (A–D) hematoxylin and eosin (H&E) staining. (E–H) Rabbit anti-Clara cell secretory protein (CCSP), (F) a more sensitive goat anti-CCSP (inset), and (I–L) β -tubulin antibodies were used to stain the tissue. After 2 days of dox, residual cuboidal cells in the bronchioles express high levels of CCSP (E, arrowhead). Two days after dox withdrawal only $4.5 \pm 2\%$ of cells express CCSP; expression in these cells is low and can be detected only with the more sensitive goat anti-CCSP antibody. Between 5 and 10 days after dox withdrawal, the percentage of CCSP-positive cells increased to $45.5 \pm 16.2\%$ and the

level of CCSP expression per cell increased (G and H, arrowheads). In the absence of cuboidal cells, squamous ciliated cells (arrowheads in I–L) covered the bronchioles. Results are representative of $n \geq 3$ triple transgenic Scgb1a1/DT-A mice.

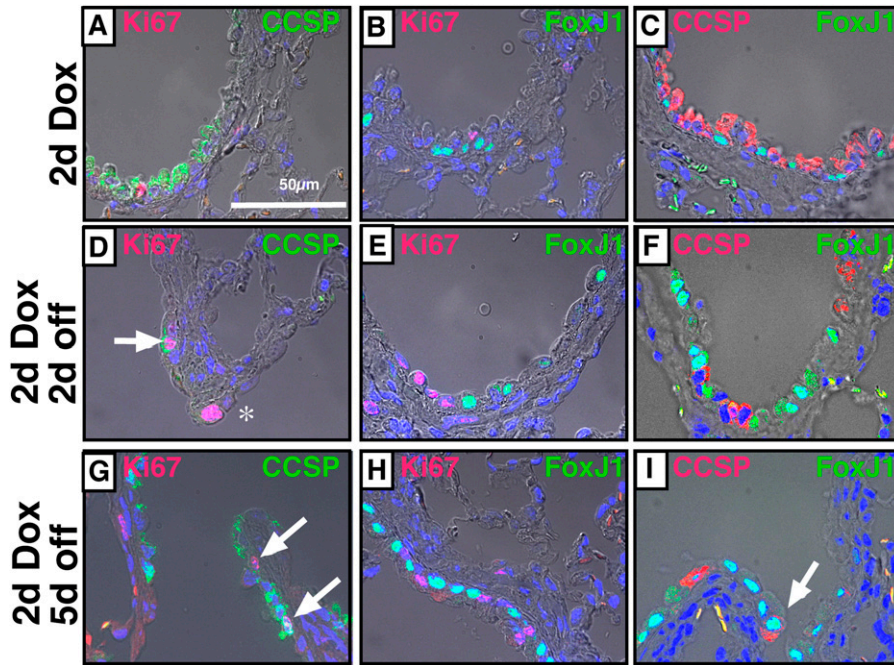


Figure 3. Cell proliferation during repair of the bronchiolar epithelium. Mice were treated with doxycycline (dox) for 2 days; proliferation was assessed after 2 days of dox treatment and 2 and 5 days of recovery, using immunohistochemistry for the proliferation marker Ki67. After 2 days of recovery $8.5 \pm 4.4\%$ of the cells were proliferative and $10.0 \pm 7.7\%$ were proliferative after 5 days. Immunofluorescence images were merged with images acquired using differential interference contrast optics: goat anti-Clara cell secretory protein (CCSP) (green in A, D, and G; red in C, F, and I), Ki67 (pink), forkhead-box J1 (FOXJ1; green). Ki67 expression was colocalized with CCSP in Clara cells but not with FOXJ1 staining (ciliated cells). Colocalization of CCSP and FOXJ1 showed a subset of dual-positive cells at 5 days but not at 2 days of recovery. Arrows, double-positive cells; asterisk, rare proliferating cuboidal cell that lacks CCSP. Results are representative of $n \geq 3$ triple transgenic Scgb1a1/DT-A mice.

niches near neuroepithelial bodies (NEBs) (6, 35). NEBs are small clusters of cells that express calcitonin gene-related peptide (CGRP) and other neuropeptides. To assess whether proliferation capacity was selectively increased in NEB-related sites, dual immunohistochemistry for CCSP and CGRP was performed on lungs after 2 and 5 days of recovery. Regenerating CCSP-positive cells were found in both NEB-associated and non-NEB-associated regions, with many NEB regions being denuded of regenerating CCSP-staining cells (Figures 4A and 4B). Morphometric analysis indicated that cell density in NEB regions was significantly increased after 2 and 5 days of recovery (Figure 4C). To assess proliferation of Clara cell progenitor cells in NEB regions, we performed dual immunohistochemistry for CGRP and Ki67. The proliferation index in bronchiolar regions with and without positive CGRP staining was determined as a percentage of Ki67-positive cells per nucleus of bronchiolar cells (Figure 4D). Morphometric analysis indicated that the proliferation index in both NEB-associated and non-NEB-associated regions of the bronchioles was comparable after 2 days of recovery and slightly elevated after 5 days of recovery (Figure 4D). Proliferation was increased in regions with higher cell density and was correlated with the presence of CCSP-positive cells. These data suggest that proliferating cells are widely distributed throughout the airways after 2 days of recovery and are associated with areas of high cell density after 5 days of recovery.

A second potential niche of airway stem cells has been identified in the bronchiolar alveolar duct junction (BADJ) region, where rare cells express both CCSP and the alveolar type II cell marker, pro-surfactant protein C (pro-SPC) (36). To assess the presence of these dual-positive cells colocalization of CCSP and pro-SPC was performed by immunohistochemistry during DT-A activation and bronchiolar recovery (Figures 4E–4H). Rare CCSP- and pro-SPC-positive cells were found only after 2 days of recovery; these cells expressed low levels of CCSP (Figure 4F). Colocalization studies with CCSP, pro-SPC, and Ki67 were assessed during repair. No colocalization of all three markers, CCSP, pro-SPC, and Ki67, was detected, suggesting that CCSP/pro-SPC dual-positive cells within BADJ

regions were not proliferative and perhaps represent an intermediate state of bronchiolar and alveolar cell differentiation.

Exhaustion of Clara Cell Progenitors

After acute Clara cell depletion, the majority of proliferative cells stained for CCSP and had repopulated $45.5 \pm 16.3\%$ of the bronchiolar epithelium within 10 days. However, although significantly more Clara cells were present after 3 weeks of recovery ($70.6 \pm 4.7\%$; $P < 0.001$), 29.4% of the bronchiolar regions still lacked CCSP-expressing cells (arrowheads in Figures 5B and 5C; Figure 6), suggesting an important role for Clara cells in the regeneration of bronchiolar epithelium. To establish a chronic injury model and to deplete existing and newly forming Clara cells, Scgb1a1/DT-A mice were treated with dox for 10 days. The extent of Clara cell depletion and repair was assessed by immunohistochemistry for CCSP after 10 days and 3 weeks (Figures 5D–5F and Figure 6A). After 10 days of dox-induced DT-A expression, the bronchiolar epithelium consisted of a thin squamous epithelial cell layer and $16.5 \pm 8.6\%$ of cuboidal cells that expressed low levels of CCSP. After 10 days of repair Clara cells had significantly repopulated bronchioles ($65.7 \pm 11.6\%$; $P < 0.001$), and thereafter the percentage of Clara cells remained the same ($57.7 \pm 6.9\%$; $P < 0.2$) (arrows in Figures 5E and 5F; Figure 6A). Large areas of squamous epithelial metaplasia persisted (arrowheads in Figures 5E and 5F). To determine whether prolonged depletion of Clara cells resulted in regional exhaustion of Clara cell progenitors and abnormal epithelial repair, lung histology was assessed 19 weeks after withdrawal from dox (Figures 5G–5I). Although Clara cells covered most bronchioles, extensive epithelial metaplasia persisted (arrowhead in Figure 5G), supporting the concept that continuous depletion of Clara cells and newly differentiating Clara cells had exhausted resident progenitor cell pools. Aberrant bronchiolar repair was evident, as clusters of Clara cells were observed inside the bronchiolar lumen (Figures 5H and 5I), thus demonstrating that continuous depletion of Clara cells triggers regional hyperproliferation of Clara cells that form aberrant epithelial clusters while other regions remain denuded of Clara cells.

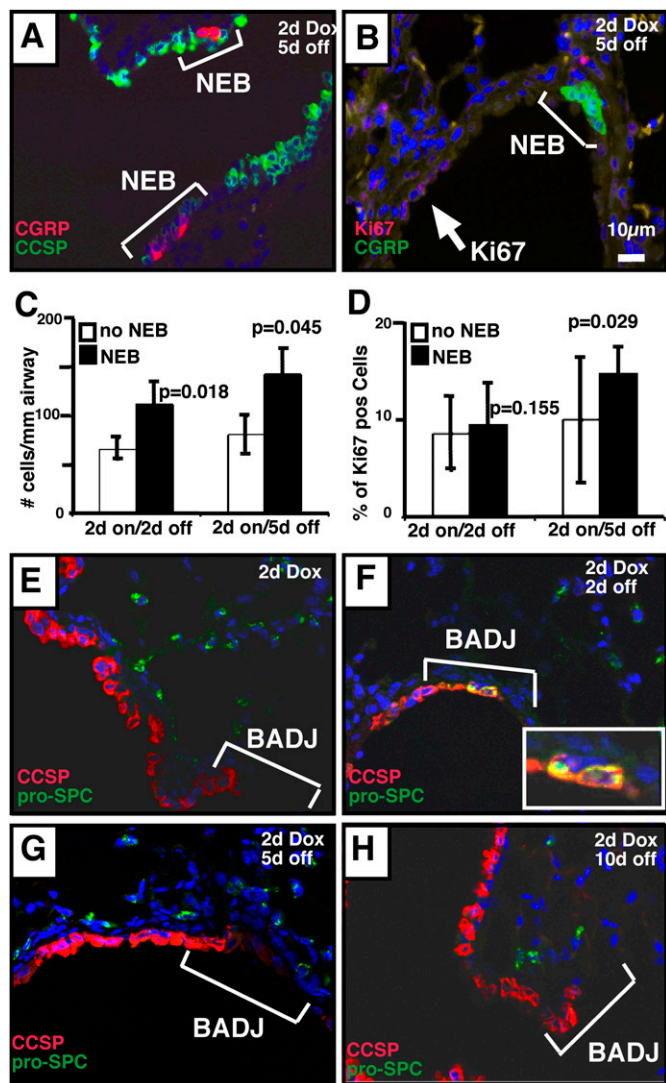


Figure 4. Assessment of proliferation in neuroepithelial body (NEB) and bronchiolar alveolar duct junction (BADJ) regions. Immunohistochemistry was performed for Clara cell secretory protein (CCSP) (green in A, red in E–H), calcitonin gene-related peptide (CGRP) (red in A, green in B), Ki67 (red in B), and pro-surfactant protein C (SPC) (green in E–H). (A and B) NEB regions were determined by positive CGRP staining and included bronchiolar cells covering the NEB and two or three cells outside the CGRP-positive area. After 2 days of doxycycline (dox) treatment and 5 days of recovery, not all NEB regions were covered with regenerating Clara cells; proliferating cells were found outside of NEB regions. (C and D) Sections containing all five lobes were double labeled for Ki67 and CGRP, and counterstained with 4',6-diamidino-2-phenylindole (DAPI). The number of DAPI-positive cells per millimeter of airway and the percentage of Ki67-positive cells per DAPI-positive cell in NEB and non-NEB regions were determined. (C) Cell density around NEB regions (solid columns) was 112 cells/mm of airway after 2 days of recovery and 143 cells/mm after 5 days of recovery, which was significantly more than the 66 and 81 cells/mm in the non-NEB regions (open columns) ($P < 0.018$ and $P < 0.045$, respectively). (D) After 2 days of recovery proliferation in NEB (solid columns; 9.5%) and non-NEB (open columns; 8.5%) regions was comparable ($P < 0.155$). After 5 days of recovery proliferation in NEB (black; 14.7%) was slightly increased when compared with non-NEB regions (white; 10.0%) ($P < 0.029$). Results are expressed as the means \pm SE of six sections of three to five animals per group. (E–H) Colocalization of goat anti-CCSP (red) and SPC (green) in the bronchiolar epithelium was assessed after acute injury and recovery for 2, 5, and 10 days. Immunofluorescence images were merged with images acquired with differential interference contrast optics. Only after 2 days of recovery were rare clusters of dual-positive cells found in BADJ regions (1 cluster per 15 BADJ regions). High magnification of a dual-positive BADJ cluster is shown in the inset in (F). Results are representative of more than 45 BADJ regions from 3 sections, containing all 5 lobes, of 3–5 triple transgenic Scgb1a1/DT-A animals per group at each time point.

Airway Wall Fibrosis after Chronic Clara Cell Depletion

Acute and chronic graft rejection after lung transplantation or bone marrow transplantation causes inflammation and bronchiolar fibrosis, known as bronchiolitis obliterans syndrome (9). To assess the potential effect of chronic Clara cell depletion on the induction of bronchiolar fibrosis, mice were treated with dox for 10 days. Continuous depletion of Clara cells for 10 days caused thickening of the peribronchiolar stroma at sites associated with squamous epithelial metaplasia. Morphometric analysis determined that the average thickness of the mesenchyme adjacent to the basement membrane increased significantly from 4.8 ± 0.3 to $12.6 \text{ mm}^2/\text{mm}$ of airway ($P < 0.001$) (Figure 6B) after chronic injury. Peribronchiolar fibrosis persisted throughout 10- and 21-day recovery periods with thickening of 14.1 ± 0.2 and $14.4 \pm 0.1 \text{ mm}^2/\text{mm}$, respectively ($P < 0.14$) (arrowheads in Figures 5D–5F; Figure 6B). After 19 weeks of recovery, peribronchiolar fibrosis was associated with bronchioles in which Clara cells had regenerated (arrows in Figures 5G and 5H), demonstrating that peribronchiolar fibrosis was nonreversible in spite of substantial epithelial regeneration.

To further characterize the peribronchiolar fibrosis and fibrotic lesions, immunohistochemistry was performed with markers for specific cell types and for cell proliferation (Figures 7A–7D). Trichrome staining was used to assess extracellular

matrix deposition (Figure 7E). After 10 days of dox treatment, followed by either 2 or 10 days of recovery, the peribronchiolar thickening was most prominent at sites of squamous epithelium that lacked both Clara and ciliated cells (Figures 7A and 7B). Fibrotic regions contained proliferating fibroblasts, capillaries, extracellular matrix, and collagen (Figures 7C–7E), thus resembling fibromyxoid plugs of granulation tissue. Because an increase in myofibroblast activity has been found in animal models of pulmonary fibrosis (37, 38), we performed immunohistochemistry for α -smooth muscle actin (α -SMA). The smooth muscle layer was not increased in these fibrotic areas (Figure 7F). These data support the concept that peribronchiolar fibrosis was associated with proliferating fibroblasts and deposition of extracellular matrix but was not associated with peribronchiolar smooth muscle hyperplasia, suggesting that fibrosis was independent of myofibroblast proliferation or differentiation.

Investigation of EMT

In many adult tissues, epithelial cells respond to stress or injury by a dedifferentiation process termed the epithelial-mesenchymal transition (EMT) (17). To evaluate whether EMT contributed to the peribronchiolar fibrosis after chronic Clara cell ablation we assessed immunohistological markers associated with EMT (39). After 10 days of dox treatment, areas with moderate peribronchiolar fibrosis (Figure 8) and intrabronchiolar fibrotic lesions were compared (Figure 9). Regions with

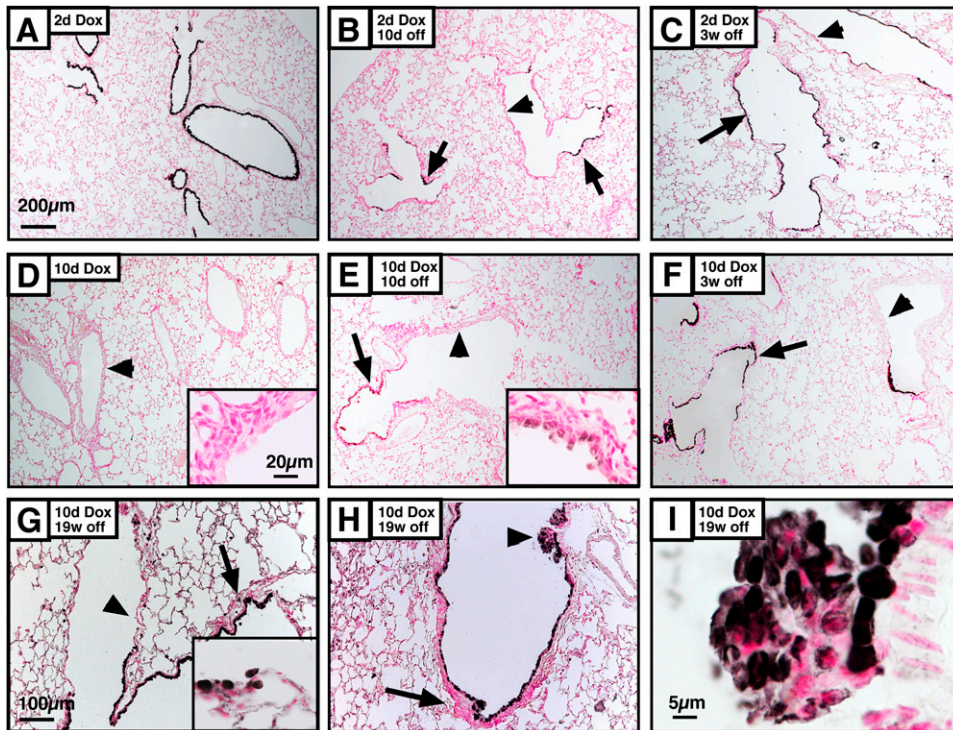


Figure 5. Chronic loss and aberrant repair of Clara cells after continuous diphtheria toxin A (DT-A) expression. Immunohistochemistry for Clara cell secretory protein (CCSP) was assessed on lung sections of triple transgenic Scgb1a1/DT-A mice after 2 days (A–C) or 10 days of DT-A expression (D–F), and recovery for (B and E) 10 days, (C and F) 3 weeks, and (G–I) 19 weeks. After 3 weeks of recovery Clara cells lined many bronchioles (arrows) but were absent in some bronchiolar regions. After 19 weeks of recovery, some bronchioles still lacked Clara cells (arrowheads in B–G). Peribronchiolar fibrosis was found after 10 days of doxycycline (dox) treatment (insets in D and E) and persisted throughout 19 weeks of recovery (arrows in H). After 19 weeks of recovery, aberrant epithelial repair was evident (H). Scale bars: (A–F) 200 μ m; (G and H) 100 μ m; (I) 5 μ m. Results are representative of $n \geq 3$ triple transgenic Scgb1a1/DT-A mice.

moderate airway wall thickening were covered by a thin, squamous epithelium that stained for pan-cytokeratin and lacked N-cadherin (Figures 8A and 8B). Fibrotic lesions growing into the bronchiolar space were associated with regions that lacked epithelial cells, as indicated by the absence of pan-cytokeratin (Figure 9A). Morphometric analysis revealed that after acute injury 0.5–2.5% of bronchiolar epithelium was denuded whereas 6–28% was denuded after chronic injury. N-cadherin expression, normally absent in bronchioles, was induced in epithelial cells adjacent to the intrabronchiolar lesions (Figure 9B), suggesting a more migratory phenotype for these epithelial cells (40). Collagen IV staining was detected in regions with moderate peribronchiolar fibrosis but was not seen throughout the intrabronchiolar fibrotic lesions (Figures 8 and 9C). Staining for desmin, drebrin (data not shown), α -SMA, and vimentin (Figure 8 and Figures 9D–9F) revealed that both airway wall thickening and intrabronchiolar lesions occurred in the absence of fibroblast-to-myofibroblast differentiation. Expression of the epithelial transcription factor TTF-1 (thyroid transcription factor-1) was weak and patchy, suggesting loss of differentiation or absence of epithelial cells (Figure 8 and Figures 9E and 9F). These data suggest that epithelial cells associated with peribronchiolar fibrosis (Figure 8) undergo partial dedifferentiation associated with loss of markers for differentiated epithelial cells (CCSP, TTF-1, β -tubulin) but maintain expression of pan-cytokeratin, indicating their epithelial phenotype. Complete loss of epithelial cells, as demonstrated by lack of pan-cytokeratin and N-cadherin expression, was associated with fibrotic callus formation in the airway lumen. These lesions stained positive for vimentin and platelet–endothelial cell adhesion molecule (PECAM) but lacked α -SMA, suggesting granulation tissue formation after loss of the bronchiolar epithelium. Staining for SNAIL, SLUG, and TWIST, transcription factors associated with EMT, was not detected in regions of peribronchiolar fibrosis or intrabronchiolar lesions during acute or chronic injury or during recovery periods (Figure 10).

DISCUSSION

In this study, we have shown that Clara cells are critical airway progenitor cells and that chronic Clara cell depletion resulted in exhaustion of bronchiolar progenitor cell pools and peribronchiolar fibrosis (Figure 11). Evidence that the Clara cells are an important progenitor cell population has been demonstrated in two ways. First, proliferation during epithelial repair was associated primarily with Clara cells that expressed low levels of CCSP and was not found in ciliated cells or in dual-positive CCSP- and pro-SPC-expressing cells in the BADJ regions. In our system proliferating cells were widely distributed along the airways and were not selectively associated with NEBs or the BADJ regions. Increased proliferation of Clara cells in the hyperplastic regions, which was seen after DT-A-mediated Clara cell depletion in line 1, supports the concept that Clara cells are important progenitor cells of the bronchiolar epithelium (2, 6, 7, 35).

Second, we found that continuous depletion of Clara cells resulted in ineffective epithelial repair, resulting in chronic squamous epithelial metaplasia and peribronchiolar fibrosis. Peribronchiolar fibrosis was associated with increased proliferation of fibroblasts, reduced expression of the epithelial marker TTF-1, and induction of N-cadherin and vimentin. At the time points analyzed and with the methods used, we could not detect expression of EMT-related transcription factors (SNAIL, SLUG, TWIST) or colocalize epithelial and mesenchymal markers. Detection of these EMT markers might have been limited by the sensitivity of the antibodies and the short time frame during which these proteins are expressed. Moreover, EMT is a transient process and colocalization of epithelial and mesenchymal markers in the same cells is rare and difficult to demonstrate. Therefore the origin of the fibroblasts in these lesions remains unclear at present. Focal loss of epithelial integrity was associated with lack of pan-cytokeratin expression, intrabronchiolar lesions, and increased proliferation of subepithelial fibroblasts. These data support the concept that loss of epithelial integrity and fibroblast proliferation cause the fibrotic

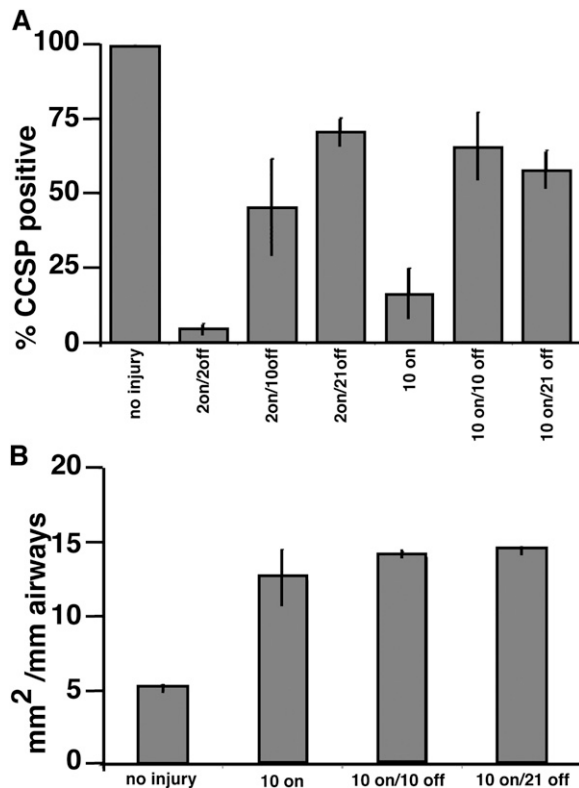


Figure 6. Extent of Clara cell depletion and mesenchymal fibrosis. Random sections from two or three animals and containing all five lobes were stained for Clara cell secretory protein (CCSP). Pictures of all airways were taken. (A) The length of total airways and CCSP-positive airways was determined. Clara cell depletion was expressed as the percentage of airways covered with CCSP-positive cells. In airways with no injury CCSP stain covered 100% of the airways. After 2 days of doxycycline (dox) and 2 days off dox treatment only $4.5 \pm 2.0\%$ of the airways were covered with Clara cells. After 10 days Clara cells significantly regenerated to cover $45.5 \pm 16.3\%$ of the bronchioles ($P < 0.001$) and continued to significantly regenerate to cover $70.6 \pm 4.7\%$ after 21 days of recovery ($P < 0.001$). After 10 days of dox $16.5 \pm 8.6\%$ of the airways were CCSP positive, which is comparable to denudation after 2 days ($P < 0.06$). Ten days after chronic injury Clara cells regenerated and covered $65.7 \pm 11.6\%$ ($P < 0.001$) of the airways. Thereafter the percentage of Clara cells did not increase ($57.7 \pm 6.9\%$; $P < 0.20$). (B) The area of mesenchymal tissue adjacent to the bronchiolar basement membrane was determined in uninjured bronchioles and after 10 days of dox exposure. The extent of fibrosis was determined as millimeters squared per millimeter of airway. In uninjured animals the average size of the underlying mesenchyme was $4.8 \pm 0.3 \text{ mm}^2/\text{mm}$ of airway. After 10 days of injury the mesenchyme increased in thickness to $12.6 \pm 2.0 \text{ mm}^2/\text{mm}$ ($P < 0.001$) and remained at 14.1 ± 0.2 and $14.4 \pm 0.1 \text{ mm}^2/\text{mm}$ after 10 and 21 days of repair ($P < 0.39$). Results are expressed as means \pm SE of 80–160 mm of airway from two or three animals per group.

process, associated with chronic DT-A-mediated Clara cell depletion.

Clara Cell Progenitors Are Not Selectively Associated with BADJ Regions or NEBs

Nonciliated bronchiolar epithelial cells are thought to repair the bronchiolar epithelium after injury (2–4), as previously reported in lineage-tracing studies (7, 41, 42) and studies inactivating Sox2, a transcription factor associated with stem cell behavior (8, 43), supporting the concept that basal cells and Clara cells

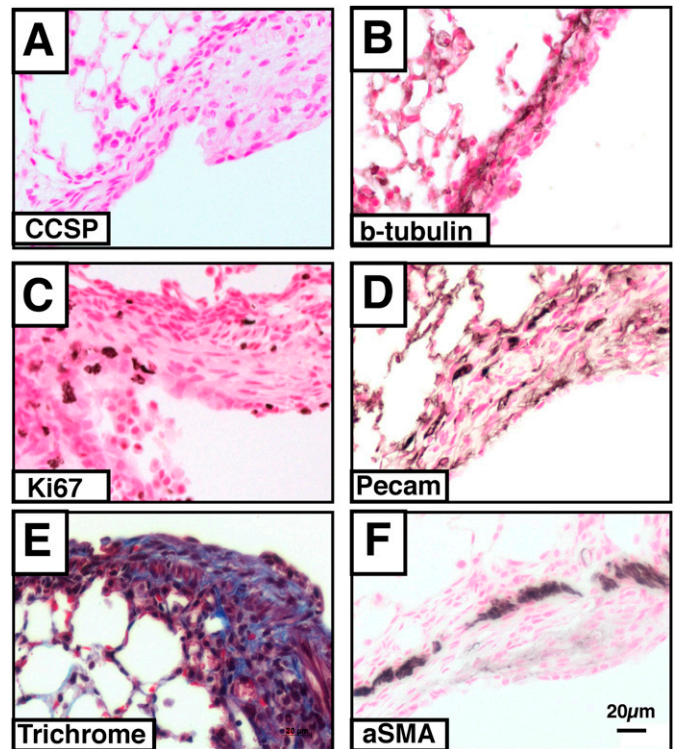


Figure 7. Chronic Clara cell depletion results in peribronchiolar fibrosis. After 10 days of doxycycline (dox) treatment, immunohistochemistry on lung sections of triple transgenic mice for cell type-specific markers was performed with (A) goat anti-Clara cell secretory protein (CCSP), (B) β -tubulin, (D) platelet-endothelial cell adhesion molecule (PECAM), and (F) α -smooth muscle actin (α -SMA). Proliferation was assessed by (C) Ki67 staining and extracellular matrix deposition was assessed by (E) trichrome staining. Peribronchiolar fibrosis was associated with loss of Clara cells, proliferating fibroblasts, and deposition of extracellular matrix but was not associated with smooth muscle hyperplasia. Results are representative of $n \geq 3$ triple transgenic Scgb1a1/DT-A mice.

serve as progenitor cells for tracheal, bronchial, and bronchiolar epithelium. However, in the mouse basal cells are not found in the bronchioles (44). NO_2 and ozone selectively kill ciliated cells that are regenerated by Clara cells (45, 46). Acute Clara cell depletion after naphthalene treatment has a well-defined pattern of repair (1, 3, 6, 35, 47–50). Clara cells express cytochrome P450, which metabolizes naphthalene to a toxic intermediate causing cell autonomous death (49, 50). It remains unclear whether all Clara cells or only restricted subpopulations of naphthalene-resistant Clara cells have the capacity to self-renew, differentiate, and repopulate the conducting airway (35, 36, 51). After naphthalene injury, surviving progenitor cells are enriched in selected niches associated with tracheal-bronchial glands, BADJ regions, and NEBs (6, 35, 36, 51, 52). Clara cells located at the BADJ have been identified by coexpression of CCSP and pro-SPC and have therefore been proposed to serve as bronchiolar-alveolar stem cells (36). In the present study CCSP- and pro-SPC-expressing cells in BADJ regions did not proliferate, and the number of proliferating cuboidal cells in the NEB regions was not increased. Our results suggest that regenerating cells are not selectively associated with NEB and BADJ regions and support studies demonstrating that regenerating cells are randomly distributed throughout the airways and contribute to airway homeostasis after moderate naphthalene injury (51). The same studies, however, showed that regenera-

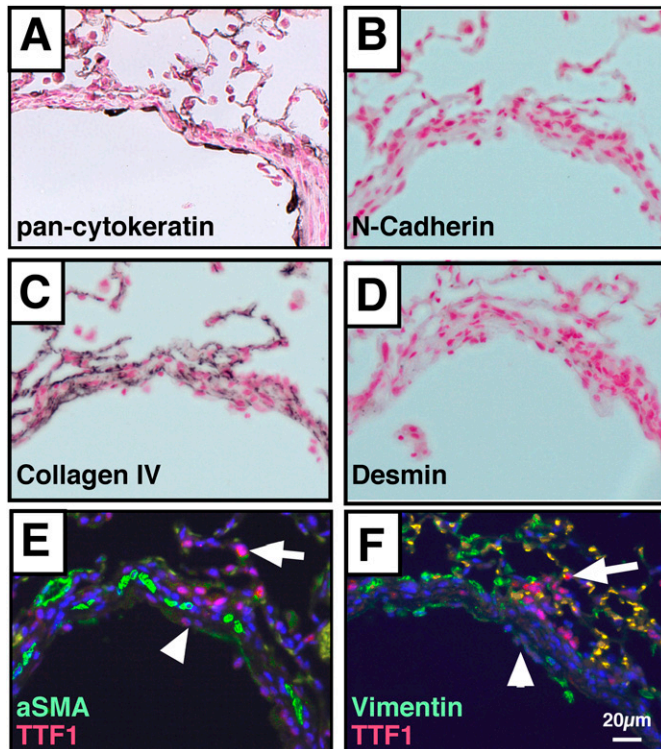


Figure 8. Immunohistochemistry (IHC) for epithelial and stromal cell markers in regions of peribronchiolar fibrosis. IHC was performed for (A) pan-cytokeratin, (B) N-cadherin, (C) collagen IV, and (D) desmin, and dual immunofluorescence was performed for thyroid transcription factor (TTF)-1 and the smooth muscle cell marker α -smooth muscle actin (α -SMA) (E) or the mesenchymal marker vimentin (F). A squamous layer of pan-cytokeratin-positive epithelial cells lined the bronchioles. Weak and patchy expression of TTF-1 suggested loss of epithelial differentiation; lack of desmin and α -SMA expression demonstrated that fibrosis was not due to myofibroblast hypertrophy. Arrows, TTF-1 expression in alveolar type II cells; arrowheads, low TTF-1 expression in squamous cells. Results are representative of $n \geq 3$ triple transgenic Scgb1a1/DT-A mice.

tion after severe naphthalene injury occurred in rare cell patches that were associated with proposed stem cell niches (35, 51).

Discrepancies between the association of progenitor cells with NEBs and BADJ regions and the random distribution of progenitor cells throughout the bronchiolar epithelium may be due to differences in how Clara cells were ablated. In the present study, Clara cells were depleted by dox-mediated DT-A activation, which depended on *Scgb1a1* promoter activity. In contrast, naphthalene injury depends on the expression of the cytochrome P450 protein, which is normally found in mature Clara cells (6). NEBs and BADJ regions harbor naphthalene-resistant variant Clara cells that express low levels of P450. Although low levels of P450 protect these cells from naphthalene injury, these cells can be ablated by the transgenic approach with the *Scgb1a1* promoter. Randomly distributed Clara cells and Clara cell progenitors that are not ablated by *Scgb1a1* promoter-dependent DT-A expression might have high levels of P450 protein expression, which allows ablation by naphthalene. Differences in the extent and type of cells targeted by conditional DT-A or naphthalene injury may account for regional differences in Clara cell depletion and subsequent regeneration in these models.

In the present study, we demonstrate that continuous depletion of newly formed Clara cells impaired regeneration of

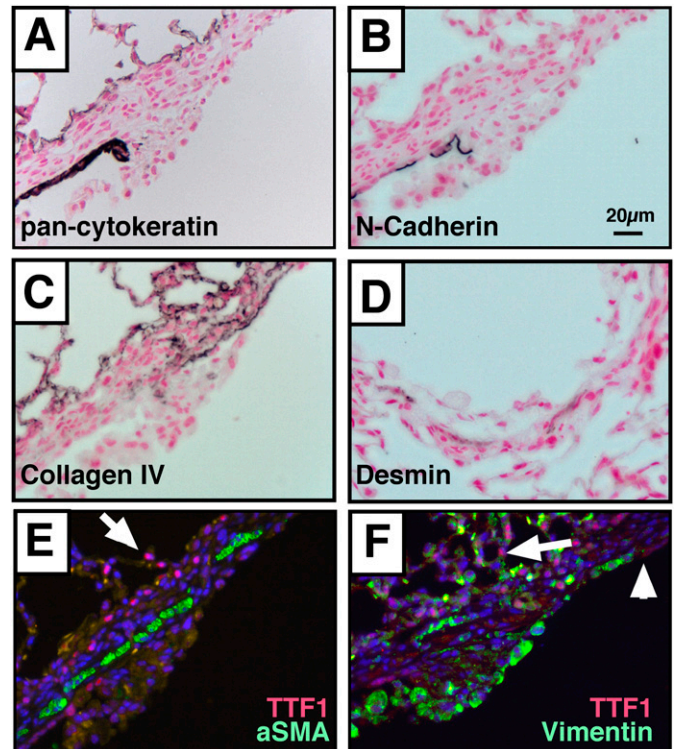


Figure 9. Immunohistochemistry for epithelial and stromal markers in regions of fibromyxoid plugs. Immunohistochemistry was performed for (A) pan-cytokeratin, (B) N-cadherin, (C) collagen IV, and (D) desmin, and dual immunofluorescence was performed for thyroid transcription factor (TTF)-1 and the smooth muscle cell marker α -smooth muscle actin (α -SMA) (E) or the mesenchymal marker vimentin (F). The epithelial layer was interrupted in regions of fibrotic callus formation, and fibrotic lesions contained vimentin-positive, α -SMA-negative fibroblasts. Arrows, TTF-1 expression in alveolar type II cells; arrowhead, low TTF-1 expression in squamous cells. Results are representative of $n \geq 3$ triple transgenic Scgb1a1/DT-A mice.

the bronchiolar epithelium and resulted in persistent squamous epithelial metaplasia and lack of Clara cell regeneration (Figure 11). These data suggest a critical role for Clara cells as progenitors of regenerating bronchiolar epithelial cells, although the progenitor of variant Clara cells and randomly dispersed Clara cell progenitors remains unclear. Although lineage-tracing studies would be useful to identify these progenitor cells, cell-specific labeling using Cre recombinase also activates DT-A in the DT-A transgenic model, and therefore results in cell death. We observed low levels of CCSP protein expression at the beginning of bronchiolar repair, indicating that this subset of Clara cells is likely derived from progenitor cells that do not have *Scgb1a1* promoter activity during dox exposure and thus do not activate DT-A. The finding that repairing regions express high levels of CCSP and could be ablated by continuous dox treatment supports this hypothesis.

Ineffective Epithelial Repair Causes Fibrosis

BOS is associated with focal denudation of the basement membrane and loss of epithelial integrity (9, 10). In the present model chronic depletion of Clara cells caused focal denudation of the basement membrane, peribronchiolar fibrosis, and regional formation of intrabronchiolar fibrotic lesions that resemble early stages of the fibromyxoid plugs found in patients with BOS. Our data support the concept that chronic epithelial loss results in ineffective epithelial repair and fibrosis by

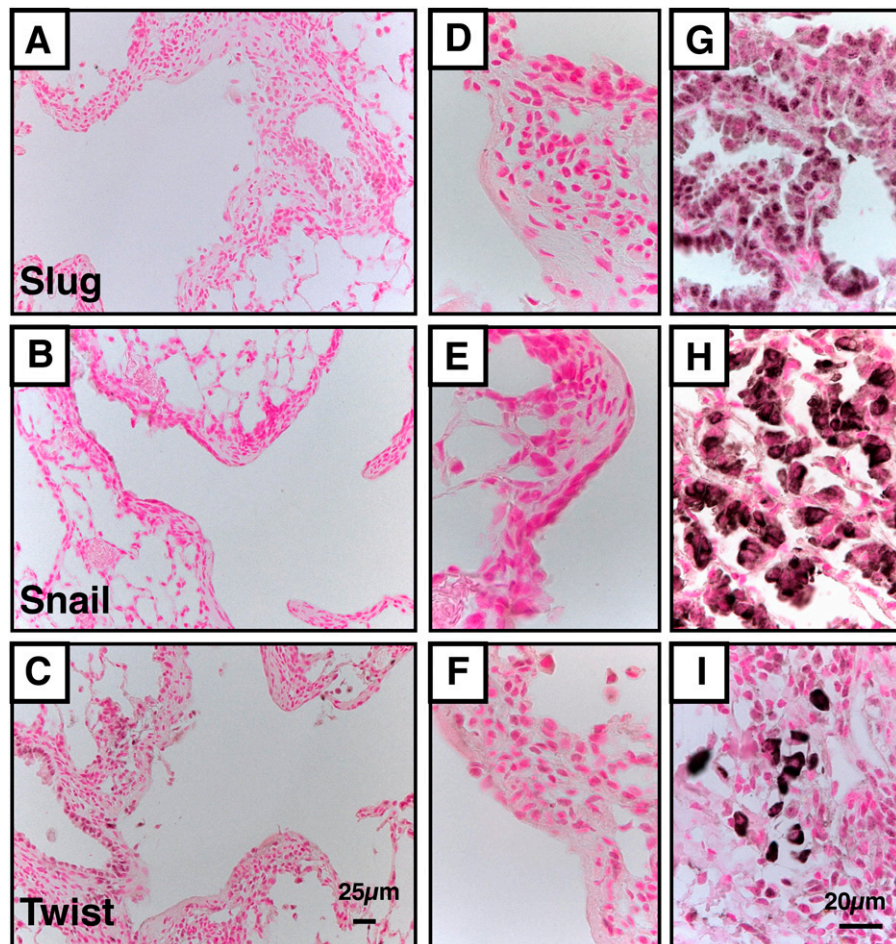


Figure 10. Lack of epithelial–mesenchymal transition (EMT) markers in fibrotic lesions. Immunohistochemistry for (A, D, and G) SLUG, (B, E, and H) SNAIL, and (C, F, and I) TWIST was performed on lung sections of triple transgenic mice after 10 days of diphtheria toxin A (DT-A) expression (A–F) and on urethane-induced lung tumors (G–I), which were used as positive controls for the antibody staining. SLUG, SNAIL, and TWIST staining was not detected in areas with peribronchiolar fibrosis or in fibrotic caluses. Results are representative of $n \geq 3$ triple transgenic *Scgb1a1/DT-A* mice at all acute and chronic injury and recovery time points.

inducing proliferation of fibroblasts and deposition of collagen. This concept is supported by lung biopsies from patients with idiopathic pulmonary fibrosis, in which cell hyperplasia, apoptosis, and chronic denudation of epithelial cells from the basement membranes were detected (53–55). Furthermore, alveolar fibrosis was induced in studies in which the murine *Sftpc* promoter was used to drive diphtheria toxin receptor and specifically deplete alveolar type II cells (16). Previously, the mouse *Scgbl1* promoter was used to drive expression of the herpes simplex virus thymidine kinase gene (CCSP-TK) in

bronchiolar epithelial cells (2). Repeated administration of ganciclovir in the CCSP-TK mouse model resulted in selective ablation of CCSP-expressing cells. However, these animals began dying 12 days after ganciclovir exposure, thus limiting studies of bronchiolar regeneration and fibrosis after chronic injury (2, 6).

We did not observe expression of SNAIL, SLUG, and TWIST, transcription factors associated with EMT, in regions of peribronchiolar fibrosis or intrabronchiolar lesions. EMT can be observed in many adult tissues, and studies support a role for

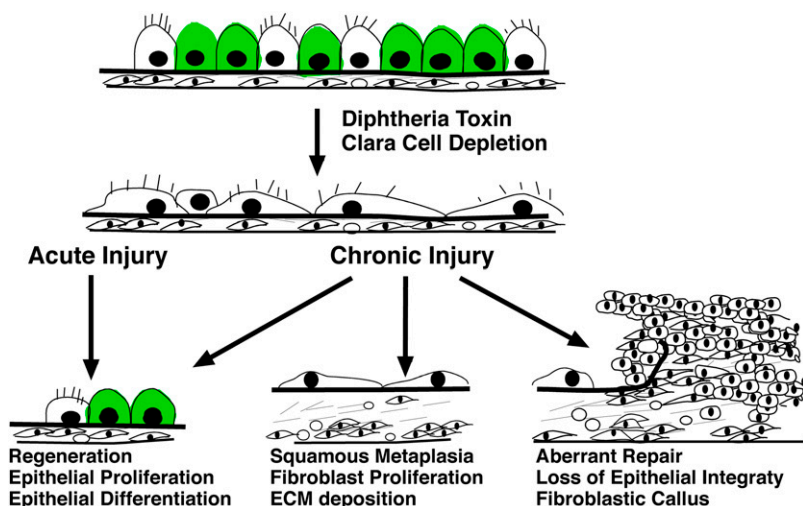


Figure 11. Schematic process of lung injury and repair after acute and chronic Clara cell depletion. Diphtheria toxin A (DT-A) was expressed in Clara cells after doxycycline (dox) treatment causing death of nonciliated cuboidal cells. After acute epithelial injury (2 d of DT-A expression), the remaining ciliated cells were squamous and covered the basement membrane. From 2 to 10 days after cessation of DT-A expression, the bronchiolar epithelium proliferated and differentiated. Acute injury did not cause stromal thickening. In contrast, after chronic injury (10 d of DT-A expression) squamous metaplasia and peribronchiolar fibrosis were observed. Squamous metaplasia, fibroblast proliferation, and excessive matrix deposition were associated with peribronchiolar fibrosis. Regional loss of epithelial integrity was associated with intrabronchiolar lesions, ineffective epithelial regeneration, and aberrant tissue repair. ECM = extracellular matrix.

EMT in response to lung injury (17). A Cre-lox approach for lineage tracing with β -galactosidase was used to demonstrate that epithelial cells undergo EMT in models of pulmonary fibrosis involving overexpression of transforming growth factor- β or insulin-like growth factor-binding protein-5 (56–58) and after administration of the chemotherapy agent bleomycin (14, 15). Lineage-tracing studies in our transgenic model are limited because cells expressing Cre are killed by the subsequent activation of the DT-A transgene, and thus the role of EMT in fibrotic peribronchiolar regions can only be ascertained indirectly. On the basis of our findings we speculate that the bronchiolar fibrosis in this model is due to proliferation of resident fibroblasts rather than transdifferentiating epithelial cells that have escaped DT-A-mediated cell death to undergo EMT. This mouse model of chronic Clara cell depletion should be useful to study the pathogenesis of fibrosis after the loss of epithelial integrity, and should facilitate studies to promote epithelial regeneration and to prevent ineffective epithelial regeneration and aberrant tissue repair.

Author Disclosure: A.-K.T.P. received more than \$100,001 from the NIH, more than \$100,001 from the AHA, and more than \$100,001 from the ALA in sponsored grants; D.R. received \$10,001–\$50,000 from Senomyx Biotech Inc in royalties for use of research materials; J.A.W. does not have a financial relationship with a commercial entity that has an interest in the subject of this manuscript.

Acknowledgment: The authors thank Dr. Susan Wert, Dave Loudy, Kristen Steinbrook, Jenna Green, Lingling Du, Chen Yin, and Jessica Kopp for technical assistance.

References

- Van Winkle LS, Buckpitt AR, Nishio SJ, Isaac JM, Plopper CG. Cellular response in naphthalene-induced Clara cell injury and bronchiolar epithelial repair in mice. *Am J Physiol* 1995;269:L800–L818.
- Reynolds SD, Hong KU, Giangreco A, Mango GW, Guron C, Morimoto Y, Stripp BR. Conditional Clara cell ablation reveals a self-renewing progenitor function of pulmonary neuroendocrine cells. *Am J Physiol Lung Cell Mol Physiol* 2000;278:L1256–L1263.
- Reynolds SD, Giangreco A, Power JH, Stripp BR. Neuroepithelial bodies of pulmonary airways serve as a reservoir of progenitor cells capable of epithelial regeneration. *Am J Pathol* 2000;156:269–278.
- Evans MJ, Cabral-Anderson LJ, Freeman G. Role of the Clara cell in renewal of the bronchiolar epithelium. *Lab Invest* 1978;38:648–653.
- Stripp BR, Sawaya PL, Luse DS, Wikenheiser KA, Wert SE, Huffman JA, Lattier DL, Singh G, Katyal SL, Whitsett JA. Cis-acting elements that confer lung epithelial cell expression of the *CC10* gene. *J Biol Chem* 1992;267:14703–14712.
- Hong KU, Reynolds SD, Giangreco A, Hurley CM, Stripp BR. Clara cell secretory protein-expressing cells of the airway neuroepithelial body microenvironment include a label-retaining subset and are critical for epithelial renewal after progenitor cell depletion. *Am J Respir Cell Mol Biol* 2001;24:671–681.
- Rawlins EL, Okubo T, Xue Y, Brass DM, Auten RL, Hasegawa H, Wang F, Hogan BL. The role of Scgbl1a1⁺ Clara cells in the long-term maintenance and repair of lung airway, but not alveolar, epithelium. *Cell Stem Cell* 2009;4:525–534.
- Que J, Luo X, Schwartz RJ, Hogan BL. Multiple roles for Sox2 in the developing and adult mouse trachea. *Development* 2009;136:1899–1907.
- Grossman EJ, Shilling RA. Bronchiolitis obliterans in lung transplantation: the good, the bad, and the future. *Transl Res* 2009;153:153–165.
- Boehler A, Estenne M. Post-transplant bronchiolitis obliterans. *Eur Respir J* 2003;22:1007–1018.
- Shapiro SD, Ingenito EP. The pathogenesis of chronic obstructive pulmonary disease: advances in the past 100 years. *Am J Respir Cell Mol Biol* 2005;32:367–372.
- Hogg JC, Chu F, Utokaparch S, Woods R, Elliott WM, Buzatu L, Cherniack RM, Rogers RM, Sciurba FC, Coxson HO, et al. The nature of small-airway obstruction in chronic obstructive pulmonary disease. *N Engl J Med* 2004;350:2645–2653.
- Selman M, King TE, Pardo A; American Thoracic Society; European Respiratory Society; American College of Chest Physicians. Idiopathic pulmonary fibrosis: prevailing and evolving hypotheses about its pathogenesis and implications for therapy. *Ann Intern Med* 2001;134:136–151.
- Aso Y, Yoneda K, Kikkawa Y. Morphologic and biochemical study of pulmonary changes induced by bleomycin in mice. *Lab Invest* 1976;35:558–568.
- Adamson IY, Bowden DH. The pathogenesis of bleomycin-induced pulmonary fibrosis in mice. *Am J Pathol* 1974;77:185–197.
- Sisson TH, Mendez M, Choi K, Subbotina N, Courey A, Cunningham A, Dave A, Engelhardt JF, Liu X, White ES, et al. Targeted injury of type II alveolar epithelial cells induces pulmonary fibrosis. *Am J Respir Crit Care Med* 2010;181:254–263.
- Willis BC, Borok Z. TGF- β -induced EMT: mechanisms and implications for fibrotic lung disease. *Am J Physiol Lung Cell Mol Physiol* 2007;293:L525–L534.
- Perl AKT, Riethmacher D, Whitsett JA. Identification of bronchiolar progenitor cells and their role in regeneration and remodeling following epithelial cell injury [abstract]. *Am J Respir Crit Care Med* 2009;179:A2388.
- Perl AK, Wert SE, Loudy DE, Shan Z, Blair PA, Whitsett JA. Conditional recombination reveals distinct subsets of epithelial cells in trachea, bronchi, and alveoli. *Am J Respir Cell Mol Biol* 2005;33:455–462.
- Whitsett JA, Perl AK. Conditional control of gene expression in the respiratory epithelium: a cautionary note. *Am J Respir Cell Mol Biol* 2006;34:519–520.
- Brockschneider D, Pechmann Y, Sonnenberg-Riethmacher E, Riethmacher D. An improved mouse line for Cre-induced cell ablation due to diphtheria toxin A, expressed from the Rosa26 locus. *Genesis* 2006;44:322–327.
- Pham CD, Yu Z, Sandrock B, Bolker M, Gold SE, Perlin MH. *Ustilago maydis* Rho1 and 14-3-3 homologues participate in pathways controlling cell separation and cell polarity. *Eukaryot Cell* 2009;8:977–989.
- Perl AK, Tichelaar JW, Whitsett JA. Conditional gene expression in the respiratory epithelium of the mouse. *Transgenic Res* 2002;11:21–29.
- Zhou L, Lim L, Costa RH, Whitsett JA. Thyroid transcription factor-1, hepatocyte nuclear factor-3 β , surfactant protein B, C, and Clara cell secretory protein in developing mouse lung. *J Histochem Cytochem* 1996;44:1183–1193.
- Snider P, Fix JL, Rogers R, Peabody-Dowling G, Ingram D, Lilly B, Conway SJ. Generation and characterization of *Csrp1* enhancer-driven tissue-restricted Cre-recombinase mice. *Genesis* 2008;46:167–176.
- Snider P, Tang S, Lin G, Wang J, Conway SJ. Generation of *Smad7^{Cre}* recombinase mice: a useful tool for the study of epithelial-mesenchymal transformation within the embryonic heart. *Genesis* 2009;47:469–475.
- Sangiorgi E, Capecchi MR. *Bmi1* is expressed *in vivo* in intestinal stem cells. *Nat Genet* 2008;40:915–920.
- Ohnmacht C, Pullner A, King SB, Drexler I, Meier S, Brocker T, Voehringer D. Constitutive ablation of dendritic cells breaks self-tolerance of CD4 T cells and results in spontaneous fatal autoimmunity. *J Exp Med* 2009;206:549–559.
- Brockschneider D, Lappe-Siefke C, Goebels S, Boesl MR, Nave KA, Riethmacher D. Cell depletion due to diphtheria toxin fragment A after Cre-mediated recombination. *Mol Cell Biol* 2004;24:7636–7642.
- Perl AK, Zhang L, Whitsett JA. Conditional expression of genes in the respiratory epithelium in transgenic mice: cautionary notes and toward building a better mouse trap. *Am J Respir Cell Mol Biol* 2009;40:1–3.
- Jung S, Unutmaz D, Wong P, Sano G, De los Santos K, Sparwasser T, Wu S, Vuthoori S, Ko K, Zavala F, et al. *In vivo* depletion of CD11c⁺ dendritic cells abrogates priming of CD8⁺ T cells by exogenous cell-associated antigens. *Immunity* 2002;17:211–220.
- Wharram BL, Goyal M, Wiggins JE, Sanden SK, Hussain S, Filipiak WE, Saunders TL, Dysko RC, Kohno K, Holzman LB, et al. Podocyte depletion causes glomerulosclerosis: Diphtheria toxin-induced podocyte depletion in rats expressing human diphtheria toxin receptor transgene. *J Am Soc Nephrol* 2005;16:2941–2952.
- Park KS, Wells JM, Zorn AM, Wert SE, Laubach VE, Fernandez LG, Whitsett JA. Transdifferentiation of ciliated cells during repair of the respiratory epithelium. *Am J Respir Cell Mol Biol* 2006;34:151–157.
- Rawlins EL, Ostrowski LE, Randell SH, Hogan BL. Lung development and repair: contribution of the ciliated lineage. *Proc Natl Acad Sci USA* 2007;104:410–417.

35. Giangreco A, Reynolds SD, Stripp BR. Terminal bronchioles harbor a unique airway stem cell population that localizes to the bronchoalveolar duct junction. *Am J Pathol* 2002;161:173–182.
36. Kim CF, Jackson EL, Woolfenden AE, Lawrence S, Babar I, Vogel S, Crowley D, Bronson RT, Jacks T. Identification of bronchoalveolar stem cells in normal lung and lung cancer. *Cell* 2005;121:823–835.
37. Moore BB, Hogaboam CM. Murine models of pulmonary fibrosis. *Am J Physiol Lung Cell Mol Physiol* 2008;294:L152–L160.
38. Hardie WD, Glasser SW, Hagood JS. Emerging concepts in the pathogenesis of lung fibrosis. *Am J Pathol* 2009;175:3–16.
39. Sabbah M, Emami S, Redeuilh G, Julien S, Prevost G, Zimmer A, Ouelaa R, Bracke M, De Wever O, Gespach C. Molecular signature and therapeutic perspective of the epithelial-to-mesenchymal transitions in epithelial cancers. *Drug Resist Updat* 2008;11:123–151.
40. De Wever O, Pauwels P, De Craene B, Sabbah M, Emami S, Redeuilh G, Gespach C, Bracke M, Berx G. Molecular and pathological signatures of epithelial–mesenchymal transitions at the cancer invasion front. *Histochem Cell Biol* 2008;130:481–494.
41. Rawlins EL, Hogan BL. Ciliated epithelial cell lifespan in the mouse trachea and lung. *Am J Physiol Lung Cell Mol Physiol* 2008;295:L231–L234.
42. Rock JR, Onaitis MW, Rawlins EL, Lu Y, Clark CP, Xue Y, Randell SH, Hogan BL. Basal cells as stem cells of the mouse trachea and human airway epithelium. *Proc Natl Acad Sci USA* 2009;106:12771–12775.
43. Tompkins DH, Besnard V, Lange AW, Wert SE, Keiser AR, Smith AN, Lang R, Whitsett JA. Sox2 is required for maintenance and differentiation of bronchiolar Clara, ciliated, and goblet cells. *PLoS ONE* 2009;4:e8248.
44. Borthwick DW, Shahbazian M, Krantz QT, Dorin JR, Randell SH. Evidence for stem-cell niches in the tracheal epithelium. *Am J Respir Cell Mol Biol* 2001;24:662–670.
45. Evans MJ, Shami SG, Cabral-Anderson LJ, Dekker NP. Role of nonciliated cells in renewal of the bronchial epithelium of rats exposed to NO₂. *Am J Pathol* 1986;123:126–133.
46. Barth PJ, Muller B. Effects of nitrogen dioxide exposure on Clara cell proliferation and morphology. *Pathol Res Pract* 1999;195:487–493.
47. Otto WR. Lung epithelial stem cells. *J Pathol* 2002;197:527–535.
48. Martin U. Methods for studying stem cells: adult stem cells for lung repair. *Methods* 2008;45:121–132.
49. Buckpitt A, Chang AM, Weir A, Van Winkle L, Duan X, Philpot R, Plopper C. Relationship of cytochrome P450 activity to Clara cell cytotoxicity. IV. Metabolism of naphthalene and naphthalene oxide in microdissected airways from mice, rats, and hamsters. *Mol Pharmacol* 1995;47:74–81.
50. Buckpitt A, Boland B, Isbell M, Morin D, Shultz M, Baldwin R, Chan K, Karlsson A, Lin C, Taff A, et al. Naphthalene-induced respiratory tract toxicity: metabolic mechanisms of toxicity. *Drug Metab Rev* 2002;34:791–820.
51. Giangreco A, Arwert EN, Rosewell IR, Snyder J, Watt FM, Stripp BR. Stem cells are dispensable for lung homeostasis but restore airways after injury. *Proc Natl Acad Sci USA* 2009;106:9286–9291.
52. Hong KU, Reynolds SD, Watkins S, Fuchs E, Stripp BR. Basal cells are a multipotent progenitor capable of renewing the bronchial epithelium. *Am J Pathol* 2004;164:577–588.
53. Morishima Y, Nomura A, Uchida Y, Noguchi Y, Sakamoto T, Ishii Y, Goto Y, Masuyama K, Zhang MJ, Hirano K, et al. Triggering the induction of myofibroblast and fibrogenesis by airway epithelial shedding. *Am J Respir Cell Mol Biol* 2001;24:1–11.
54. Kawanami O, Ferrans VJ, Crystal RG. Structure of alveolar epithelial cells in patients with fibrotic lung disorders. *Lab Invest* 1982;46:39–53.
55. Kasper M, Haroske G. Alterations in the alveolar epithelium after injury leading to pulmonary fibrosis. *Histol Histopathol* 1996;11:463–483.
56. Kim KK, Kugler MC, Wolters PJ, Robillard L, Galvez MG, Brumwell AN, Sheppard D, Chapman HA. Alveolar epithelial cell mesenchymal transition develops *in vivo* during pulmonary fibrosis and is regulated by the extracellular matrix. *Proc Natl Acad Sci USA* 2006;103:13180–13185.
57. Hardie WD, Le Cras TD, Jiang K, Tichelaar JW, Azhar M, Korfhagen TR. Conditional expression of transforming growth factor- α in adult mouse lung causes pulmonary fibrosis. *Am J Physiol Lung Cell Mol Physiol* 2004;286:L741–L749.
58. Yasuoka H, Zhou Z, Pilewski JM, Oury TD, Choi AM, Feghali-Bostwick CA. Insulin-like growth factor-binding protein-5 induces pulmonary fibrosis and triggers mononuclear cellular infiltration. *Am J Pathol* 2006;169:1633–1642.

Conditional Depletion of Airway Progenitor Cells Induces Peribronchiolar Fibrosis

Anne-Karina T. Perl

Dieter Riethmacher

Jeffrey A. Whitsett

Online Data Supplement

Results:

In this study, we compared cell type specific expression of Cre recombinase in Clara Cells in adult mice after 48 hours of dox treatment (Supplemental Fig 1). Cre expression in the bronchiolar epithelium was detected in both mouse lines, but was more widespread in line #2 (Fig.1D). Clara cell specific Cre expression was confirmed by co-immunofluorescence of Cre and CCSP, which demonstrated that adult mice of line #2 had a extensive expression of Cre recombinase in nearly all Clara cells after 48 hours of dox. (Supplemental Fig.1 B, E). Using these transgenic mice Cre expression was not detected in ciliated cells (Supplemental Fig 1C, F).

Methods

Animal experiments

The rat Clara cell secretory protein promoter (2.3 kb *Scgb1a1*-promoter) (5) drives the expression of the reverse tetracycline activator (*Scgb1a1*rtTA, also known as CCSPrtTA). In the presence of doxycycline (dox), the reverse tet activator changes its conformation and binds the tet operator sequence of the tetOCre transgene, resulting in Clara-cell-specific Cre recombinase expression (20, 22). The target sequence for Cre recombinase is a lox/stop DT-A expression cassette in the Rosa26 gene locus (R26:LacZ:DT-A). In this transgene the *lacZ* gene, which is flanked by loxP sites, is excised upon Cre recombination. As a result, the *DT-A* gene moves in frame with the Rosa26 (R26) promoter and is expressed. In triple transgenic mice dox treatment activates *DT-A* gene expression in a Clara cell type specific manner causing cell autonomous death without a bystander effect (19). Dox was given to mice in the food (625mg dox /kg chow, Harlan

Teklar, Madison, WI) and gene activation was detected as early as 16 hours after dox treatment (23). Experiments were performed on at least 5 animals of each genotype.

Mice were housed in pathogen free conditions in micro-isolation cages in accordance with federal and institutional guidelines. All transgenic mice were housed in a barrier facility, with purified air and water, and were provided with either autoclaved or irradiated food. Mice were supplied with food and water *ad libitum* and were exposed to a 12 hour light/dark cycle. Mice were routinely screened for viral and bacterial infections by placing sentinels in their used cages. All studies were conducted on adult mice (8-20 weeks) in a mixed background (FVB/N and C57BL/6).

Immunohistochemistry

Lungs were inflated and fixed overnight at 4°C. All lung samples were washed with PBS, dehydrated through a graded series of ethanol solutions and processed for paraffin embedding. Sections (5 µm) were loaded onto polysine slides for analysis.

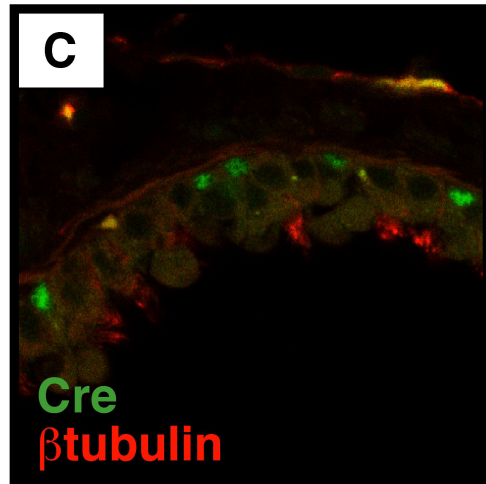
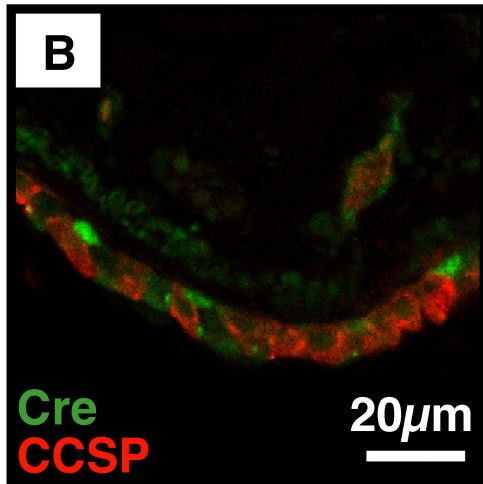
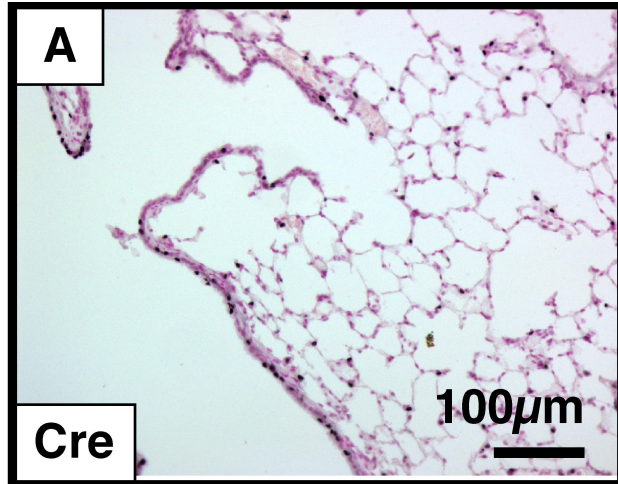
3-5 animals per group were analyzed. Fluorescence was determined by pseudo confocal microscopy using dual fluorescent labeling and a Zeiss ApoTome microscope. Images were captured using Zeiss AxioVision software and processed in Adobe Photoshop and composites were made using Macromedia Freehand. The following antibodies were used: mouse anti aSMA (IgG2A) at 1:6000, mouse anti beta tubulin IV (IgG2B) at 1:2000, rabbit anti CGRP at 1:4000, mouse anti pan-cytokeratin at 1:500, mouse anti vimentin at 1:200 (all from Sigma, St. Louis, MO); goat anti CCSP at 1:5000 (from Santa Cruz, Santa Cruz, California), rabbit anti CCSP at 1:5000, rabbit anti proSPC at 1:20000, rabbit anti TTF-1 at 1:2000 (all from Seven Hills Biolabs, Cincinnati, OH); rabbit anti Cre at 1:8000 from Novagen, Gibbstown, NJ; rabbit anti collagen IV at

1:1000, rabbit anti desmin, at 1:500, rabbit anti drebrin at 1:1000, rabbit anti N-cadherin at 1:200, rabbit anti SNAIL at 1:1000, rabbit anti SLUG at 1:500, rabbit anti TWIST at 1:100 (all from Abcam, Cambridge, MA); rabbit anti FOXJ1 a gift from Rob Costa, at 1:6000; rabbit anti phospho-histone H3 at 1:500 from United States Biological Inc., Swampscott, MA; rat anti Ki67 at 1:1000 (peroxidase) at 1:2000 (fluorescence) from Dako, Glostrup, Denmark; rat anti PECAM at 1:300 from Pharmigen, San Diego, CA. Secondary biotinylated, Alexa Fluor 488 or Alexa Fluor 594 conjugated antibodies were used at 1:200 from Molecular Probes, Invitrogen, Carlsbad, CA. Trichrome staining (Poly Scientific, Bay Shore, NY), was used according to the manufacture's recommendations.

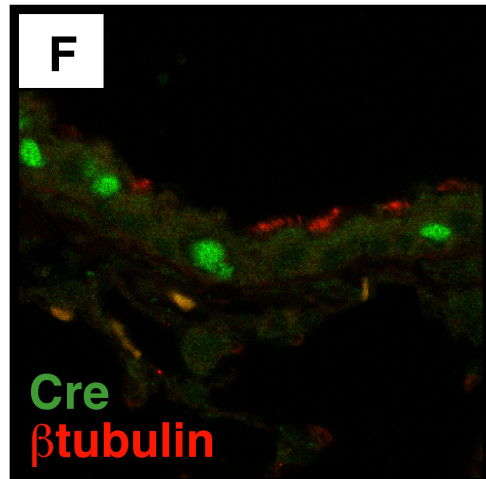
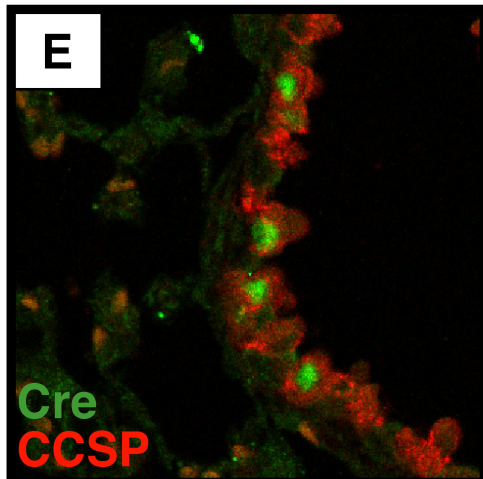
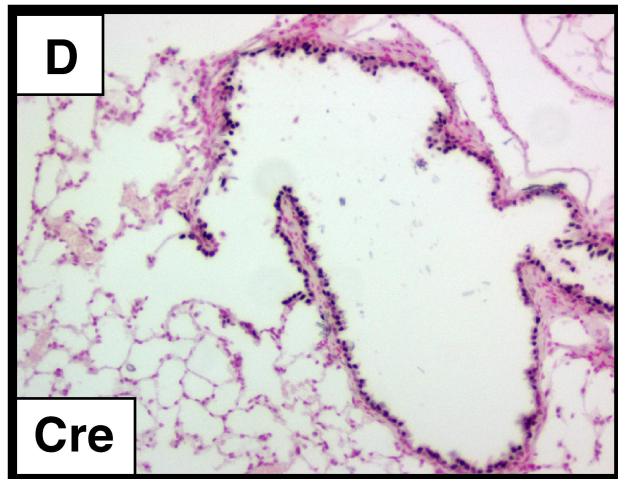
Supplemental Figure E1: Comparison of the extent of Cre expression in Scgb1a1rtTA line #1 and line #2. A, D: Immunohistochemistry for Cre protein detects expression in the epithelial cells in the bronchioles of both lines, and in alveolar type II cells in line #1 (arrow). Most Clara cells expressed Cre in line #2, while the extent of Cre expression was much less in line #1. B, E: Cre (green) localized with CCSP (red) expression (arrows). C, F: Immunohistochemistry for Cre (green) and beta tubulin (red) expression demonstrated the absence of Cre expression in ciliated cells. Photomicrographs are representative of $n \geq 5$ per group.

Supplemental FigureE2: Schematic drawing of the breeding strategy used to generate triple transgenic mice that induce DT-A expression upon dox treatment. Double transgenic mice for Scgb1a1rtTA and (tetO)7-CRE were crossed to R26:lacZ: DT-A mice to obtain triple transgenic mice. DT-A was activated only in Clara cells of triple transgenic mice and only in the presence of dox, resulting in ablation of Cre expressing Clara cells in the conducting airways.

CCSPrtTA line#1



CCSPrtTA line#2



**Scgb1a1-rtTA /
(tetO)₇-CRE**

R26:LacZ:DT-A



X



Scgb1a1-rtTA / (tetO)₇CRE / R26:LacZ:DT-A



**Cre expression
Recombination
Clara Cell Death**